Chemical ordering of alloy surfaces: Low-index versus vicinal surfaces

E. Le Goff, D. Le Floc'h, L. Barbier,* S. Goapper, and B. Salanon
DSM/DRECAM/SPCSI, CEA/Saclay, 91191 Gif-sur-Yvette Cedex, France

A. Loiseau
LEM-CNRS ONERA, Boîte Postale 72, 92322 Châtillon Cedex, France

(Received 30 March 2000; revised manuscript received 7 September 2000; published 13 March 2001)

Some A_3B fcc alloys undergo a chemical order-disorder phase transition. During the ordering process, four types of domain appear within the bulk, separated by antiphase boundaries (APB's). As for chemical ordering in the presence of a surface, scanning tunneling microscopy and He diffraction studies consistently show a contrasting behavior between vicinals, where APB's emerge at the surface, and low-index surfaces, where no APB's emerge. These differences emphasize the role of the step density in surface chemical ordering.

DOI: 10.1103/PhysRevB.63.125418 PACS number(s): 68.35.Md, 61.66.Dk, 68.35.Rh

I. INTRODUCTION

Three stages can be distinguished in the chemical ordering process of ordered alloys: in the low-T ordered phase, the symmetry of the high-temperature phase is broken and the ordered phase nucleates randomly in the bulk (nucleation stage). Upon aging below T_c, these domains grow until the full volume is ordered and sharp antiphase boundaries (APB's) are formed between domains belonging to the several possible variants (growth stage). A domain structure results and upon further aging it is followed by the coarsening of the domains (coarsening stage). After several decades of investigations, understanding of the coarsening regime of chemical ordering has been greatly improved by the work of Allen and Cahn (AC) on Fe_3Al alloy.[1] This compound undergoes a second-order bulk order-disorder phase transition. When crossing the transition, the relevant order parameter associated with chemical order decays continuously and falls to zero at the critical temperature T_c. The kinetics of coarsening below T_c is thermally activated and, as shown by AC, is driven by the thermal diffusion (function of the absolute temperature T) and not by the value of the order parameter [function of the interval $(T-T_c)$]. According to the standard AC theory, the typical domain size during the coarsening stage varies with aging time t according to the scaling law $A(T)t^{1/2}$. This dependence was shown to be related to the reduction of the curvature of the APB's. It is presumably valid for all ordering processes when the order parameter is not conserved across the transition.[2,3] The $t^{1/2}$ power law has been widely observed for bulk chemical ordering of A_3B (fcc $L1_2$) alloys of the Cu_3Au type.[4–7] Such alloys exhibit a first-order phase transition; there are four possible variants of chemical order which give rise to three different types of APB (see Fig. 1). Very recent investigations of Cu_3Au with the tomographic atom probe give evidence that the time evolution of the ordered domain size follows the very same $t^{1/2}$ law even before domains come into contact (growth regime).[7]

Chemical order-disorder transitions in the presence of a surface have attracted attention as specific surface phenomena have been pointed out.[8–12] Indeed, surface wetting by disorder below T_c was evidenced on Cu_3Au (001), for which it was found that the disordered layer thickness diverges as $\ln(T_c-T)$.[8] Wetting by disorder is a common property of two-dimensional interfaces and has also been observed at APB's in bulk Cu_3Au,[8,9] and Cu-Pd(17%).[13] In addition, the surface composition is altered as compared to that in the bulk due to segregation phenomena. As a consequence, it was shown, for example, that as little as 3% excess Au concentration lowers the temperature of the bulk transition $[T_c(Cu_{72}Au_{28})=644.5\,K]$ whereas, due to surface segregation, the surface transition is 20 K higher.[14]

As for chemical ordering kinetics in the presence of a surface, McRae and Malic[11] showed an initial surface ordering prior to bulk ordering in Cu_3Au. Reichert *et al.*[10] pointed out in x-ray experiments on Cu_3Au (001) a strongly anisotropic ordering and found that no APB's with a component of the translation vector perpendicular to the surface plane (as defined in Fig. 1) are created in the surface region. In contrast, a high APB density within the surface plane has been observed when the vicinal surface Cu-Pd(17%) (1,1,11) is briefly annealed below T_c.[12] While both alloys belong to the same cubic crystallographic class (fcc$L1_2$), one can

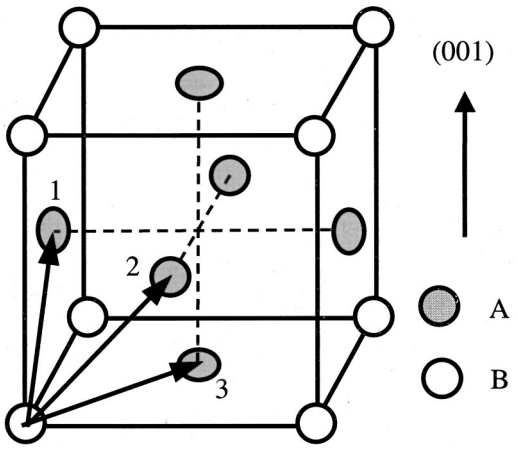

FIG. 1. Unit cell of an ordered A_3B alloy. The three numbered arrows indicate the vectors of translation between the four different variants of the chemical structure. Each translation vector defines one type of APB. The 1 and 2 translations induce a phase shift in the concentration profile in the (001) (z) direction.

wonder whether it is the nature of the alloy or the surface orientation (flat/vicinal surface) that is responsible for these different behaviors. Indeed, the two alloys differ in various aspects.

(1) For the surfaces, experiments have shown that the terminal plane of a (001) surface is pure Cu for Cu-Pd(17%) whereas the termination is mixed Cu-Au for Cu_3Au.[15]

(2) For Cu-Pd(17%), bulk APB's exhibit no strong preferential orientation[13] whereas APB's of Cu_3Au are predominantly oriented in the low-index {001} planes.[16,17] This difference can be related to the different ratio between first- and second-nearest-neighbor interactions. When the nearest-neighbor interaction is dominant, conservative APB's (for which the number of *A* and *B* nearest-neighbor atoms is conserved) have a low creation energy and faceting of APB's along {001} planes results. For the same reason, the anisotropy of the short-range order above T_c is much higher for Cu_3Au than for Cu-Pd(17%).[18] As a consequence, it has been noted by Cahn[19] that the anisotropy of the APB's as observed in Cu_3Au makes chemical ordering for this alloy more complex.

Interactions and surface segregation for the two alloys are notably different. It would be highly desirable to determine whether the observed behaviors in surface chemical ordering (the presence or absence of APB's in the surface plane) can be linked to the presence of steps. In order to answer this question, we have investigated a vicinal surface of Cu_3Au (001) and the (001) surface of Cu-Pd(17%). Scanning tunneling microscopy (STM) and He diffraction techniques have been used to determine surface morphologies. The full set of experimental data [previous results on Cu_3Au (001),[10] and Cu-Pd(17%) (1,1,11),[12] together with the present results on a vicinal of Cu_3Au (001) and on Cu-Pd(17%) (001)] allows us to propose an overall scheme for chemical ordering at surfaces, able to reconcile the experimental observations.

II. EXPERIMENT

One Cu-Pd(17%) and one Cu_3Au (composition 26.75 at. % Au) single crystals were used. The concentration of the Cu-Pd alloy differs from the ideal A_3B stoichiometry and corresponds to the congruent point.[20] We thus avoided the two-phase regions as well as the long-period structures (for higher Pd concentrations) in the phase diagram. In Cu-Au, the congruent point is reached for the stoichiometric alloy Cu_3Au. The as-grown Cu_3Au crystal was found to exhibit a slightly higher concentration. We have checked that this does not induce the formation of long-period APB structures at low temperature. In addition, similar experiments on a sample with a lower Au concentration (24.23 at. % Au) showed that a small variation of the concentration does not alter the present results.[21]

The lattice parameter for the Cu-Pd(17%) crystal is $a_0 = 0.367$ nm, the related elementary step height is $h = a_0/2 = 0.184$ nm, and the nearest-neighbor distance within (001) terraces is $a = 0.260$ nm. The temperature for the chemical order-disorder transition is $T_c = 778$ K. Data for Cu_3Au are $a_0 = 0.375$ nm, $h = 0.187$ nm, $a = 0.265$ nm, and $T_c = 663$ K. For the Cu_3Au vicinal surface, the (1,1,13) [vicinal of (001), miscut $(6.2 \pm 0.3)°$] orientation was chosen to have a high density of interacting steps while keeping wide enough terraces, which enables a straightforward interpretation of He diffraction spectra and easy STM imaging. Single crystals were aligned by the Laue technique ($\pm 0.2°$) and the samples (typically 12 mm in diameter, 2 mm thick) were spark cut. After mechanical and electrochemical polishing, the surface of the crystals were Ar^+ sputtered (400 eV, 6 μA, 1 h at room temperature) under ultrahigh vacuum. Preferential sputtering [Cu for Cu-Pd(17%), Au for Cu_3Au] is observed by Auger electron spectroscopy. Before He diffraction and scanning tunneling microscopy experiments, brief annealing at 800 K enables restoring the surface stoichiometry before ordering below T_c. He diffraction and STM experiments were performed in different vacuum chambers. Our He diffractometer has been described elsewhere.[22] The energy and wave vector of the incident beam are, respectively, $E = 22.1$ meV and $K = 65$ nm^{-1}. Our commercial STM (Omicron 1) allows imaging at room temperature after quenching from the ordering temperature.

III. VICINALS OF Cu_3Au AND Cu-Pd(17%)

A. Equilibrium structure

Owing to the bulk structure the (001) and (110) crystallographic planes of A_3B fcc $L1_2$ crystals are alternately pure *A* and mixed *AB*. The chemical order can be described by a three-component order parameter (η_x, η_y, η_z). The *z* direction designates the normal to the surface. The ideal cut of the bulk with a small angle (miscut α) with respect to (001) would exhibit steps separated by *A* or *AB* terraces. This structure is shown in Fig. 2 for the (1,1,11) surface [vicinal of (001), nominal miscut $\alpha = 7.33°$, average terrace width $L_0 = 5.5a$, step-to-step distance $L = |\mathbf{L}_0 + \mathbf{h}|$]. This morphology is unstable and STM images of Cu_3Au (1,1,13) (Ref. 21) and Cu-Pd(17%) (1,1,11) (Ref. 23) after long aging treatments show paired steps separated by double-width terraces as shown in Fig. 3. Similar paired-step morphology has been observed for a vicinal of Cu-Pd(17%) (110).[24] For both alloys, the paired-step structure in the ordered phase reverts to a single-step structure in the disordered phase ($T > T_c$). The single-step distribution ($T > T_c$) is even for Cu-Pd(17%) vicinals whereas single-step bunching occurs for Cu_3Au (1,1,13).[21]

B. Cu_3Au (1,1,13) ordering

As shown in Fig. 4, STM images of the Cu_3Au (1,1,13) sample show surface domains defined by step pairing. As there are two ways to pair adjacent steps the surface exhibits two types of variant. From one surface domain to the next, paired steps separate to be paired in the other way. Changes in pairing thus define surface antiphase boundaries (SAPB's) as shown in the scheme of Fig. 4.

After 18 h annealing at $T_c - 20$ K, wide surface domains are visible. Inside a given domain, the surface structure exhibits pairs of steps; the distance between the two steps is mainly $0.5a$ or $1.5a$ (Fig. 3) and rarely $2.5a$. According to the bulk structure, and to the following observations on

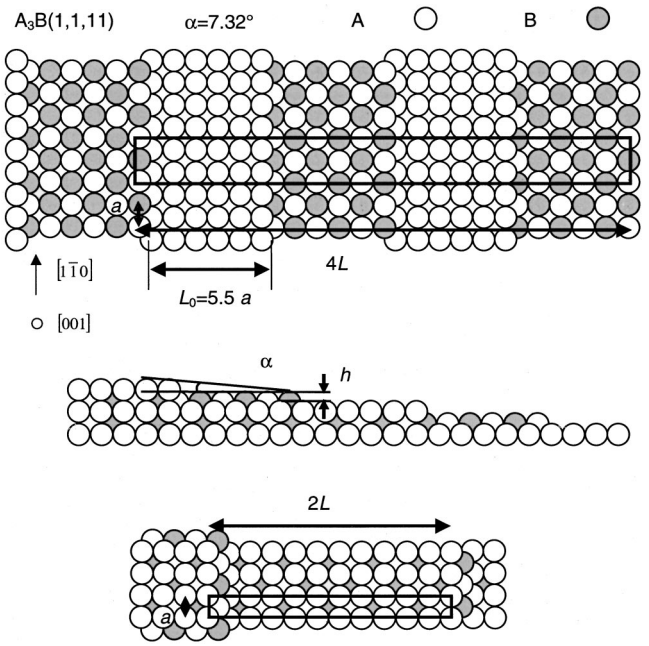

FIG. 2. Top: top view of the bulk truncation along the (1,1,11) orientation ($L_0=5.5a$) of a chemically ordered $L1_2$ A_3B alloy. The heavy rectangle indicates the centered surface unit cell. Middle: side view of the same structure. Bottom: top view of the paired-step structure with pure A terraces. The heavy rectangle indicates the surface unit cell as observed by He diffraction.

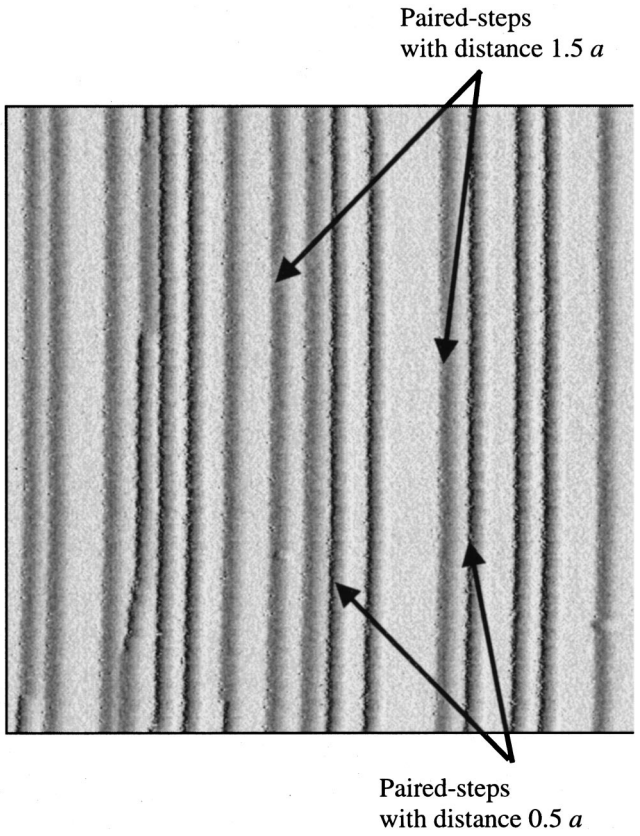

FIG. 3. $\partial z/\partial x$ STM picture (52 nm$\times$52 nm) for Cu_3Au (1,1,13). $T=300$ K, $I=0.86$ nA, $V=1.39$ V. Paired steps at minimum separation distance ($0.5a$) are seen as black vertical lines and paired steps separated by $1.5a$ as gray lines.

Cu_3Au (001) and on our STM pictures, it is very reasonable to assume that the structure of the paired-step vicinal surface is composed of terminal terraces with the mixed composition (Cu-Au) whereas subterrace atomic planes are pure Cu planes. Indeed, low-energy ion scattering studies on the (001) surface have shown that the preferred bulk termination is a Cu-Au plane.[25] In addition, straight [110] double-height steps and a well-resolved CuAu terrace structure have been observed by STM on a Cu_3Au sample cut 2° off the [001] direction.[26] Some of our STM images where atomic resolution along step edges is obtained (see Fig. 5) support our assumption on the nature of the emerging atomic planes. On these images, the tip-height modulation along the upper step edge ($A1$-$A2$) is high with a wavelength of 0.53 nm, i.e., twice the nearest-neighbor distance a. One atom out of two is seen. At the lower step edge ($A'1$-$A'2$) the modulation is much weaker with a wavelength comparable with the atomic distance of 0.26 nm (equal to a; all atoms are seen). Finally, it must be noted that the surface structure considered is similar to the one we observed on Cu-Pd(17%) (1,1,11),[12] except that the role of mixed and pure Cu planes is reversed.

As has been shown for Cu-Pd(17%) (1,1,11),[12] the SAPB's can be interpreted as being caused by the emergence of bulk APB's (see the scheme of Fig. 6). The STM image shown in Fig. 7, where one SAPB crosses the steps as seen by the change in step pairing, supports this assumption. The cross sections along upper step edges ($A1$-$A2$, $B'1$-$B'2$, or $D1$-$D2$) exhibit a wavelength of the tip-height modulation of $2a$. At lower step edges ($A'1$-$A'2$, $B1$-$B2$, and $C1$-$C2$) the modulation has a lower amplitude, as in the image of Fig. 5 (the associated wavelength is, however, hardly seen in this image, where a lower resolution was reached). This is consistent with a change in the nature of A and B step edges when crossing the SAPB. All SAPB's observed with atomic resolution exhibit such changes in tip-height modulation at step edges. These observations confirm that the near-surface chemical domain structure becomes apparent via the step domain structure. As SAPB's, separate adjacent domains with shifted concentration along the [001] direction, it is noticeable that only two APB's out of three can be seen in that way.

The coarsening of the surface domains was investigated by STM. Images were recorded at room temperature after annealing at T_c-20 K for different times, which shows the time evolution of the domain distribution (see Fig. 8). For short annealing time, no strong preferential orientation of the SAPB's is observed, whereas after 18 h annealing one sees that SAPB's are predominantly aligned along the [100] and [010] directions. The very same behavior was observed by electron microscopy for bulk APB's.[16,17]

The characteristic surface domain size Λ was measured for each annealing time. At least 10 images (102.4 nm $\times$102.4 nm) like those shown in Fig. 8 were analyzed. For this purpose, the total length d of the SAPB's for a total surface S is measured for each set of images and Λ is obtained as

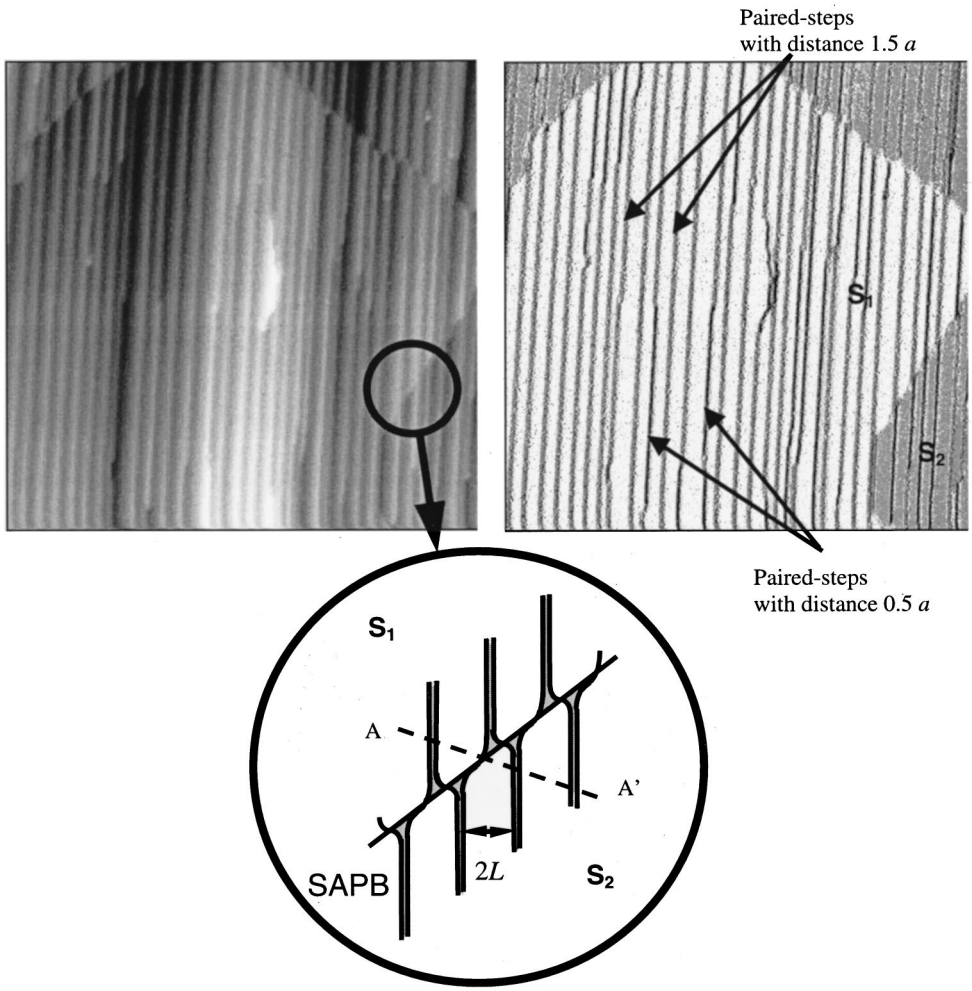

FIG. 4. Top left: Cu_3Au (1,1,13) STM image (102.4 nm×102.4 nm) after 18 h annealing at T_c 20 K. Two domains for step pairing are seen. Top right: $\partial z/\partial x$ image of the same area allows the steps to be seen better. Terraces belonging to one surface domain (S_2) have been colored in dark gray. Within the central surface domain S_1, steps separated by 0.5a and 1.5a are seen. Bottom: scheme of the step configuration close to a SAPB (white terraces, CuAu; gray terraces, Cu). The subsurface structure along AA' is given in Fig. 6 below.

$$\Lambda \approx \frac{2S}{L}. \tag{1}$$

Results are given in Fig. 9. For long aging time, the values of Λ are close to the size of bulk domains as measured by x-ray diffraction for the same temperature range by Hashimoto, Nishimura, and Takeuchi[5] and by Poquette and Mikkola.[4] These authors find a $t^{1/2}$ AC-type dependence. For short aging time, Λ is much larger than the bulk domain size. Two reasons may explain this difference. First, domains smaller than a few double-terrace widths may not be seen through the step pairing. Second, it may happen that ordering is faster near the surface, which would increase the size of surface domains with respect to those in the bulk in the very early stages of ordering and coarsening.

C. Comparison with Cu-Pd(17%)

1. Cu-Pd(17%) (1,1,11)

Results obtained for the Cu_3Au (1,1,13) surface can be compared to those of our previous STM and He diffraction studies on a vicinal of Cu-Pd(17%) (001).[12] In the following, we briefly recall the main results for this surface in order to point out the similarities between the two systems.

A surface domain structure similar to that of Cu_3Au was observed on Cu-Pd(17%) (1,1,11).[23,27] Step pairing occurs on the latter surface in such a way that terraces are always pure Cu, which is found to be the preferential termination for (001) terraces. Chemical ordering of this surface can be deduced from the evolution of SAPB's.[12] At crossing points with SAPB's, paired step separate to be paired in the other way, whereas step edges are found to change from pure Cu to Cu-Pd. As for Cu_3Au, surface domains correspond to different variants of the $L1_2$ structure. The average domain size Λ was measured on STM images and by He diffraction versus ordering time and temperature (see Fig. 10). In the late stage of ordering, Λ is found to vary as $A(T)t^{1/2}$ in agreement with the AC scaling law (see Fig. 10). As for the vicinal of Cu_3Au, Λ is found for $T=T_c-50$ K to be close to the bulk domain size measured by x-ray diffraction. In addition, an Arrhenius plot of the prefactor $A(T)$ gives an activation energy of 2.25±0.15 eV, close to the value measured for Cu-Pd(17%) bulk ordering (2.0±0.15 eV).[12]

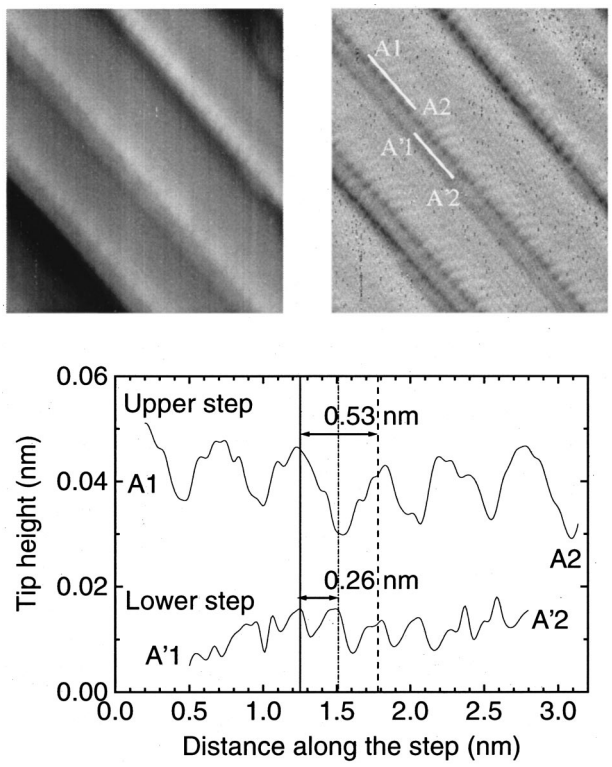

FIG. 5. Top left: 11 nm×10 nm high-resolution STM image. Top right: $\partial z/\partial x$ image of the same area. Three paired steps are seen. Bottom: tip height along upper ($A1$-$A2$) and lower ($A'1$-$A'2$) step edges. Along the upper step edge the wavelength is 0.53 nm, close to twice the nearest-neighbor distance a, and it is 0.26 nm at the lower step edge. This is consistent with a surface structure where terraces are CuAu planes over pure Cu subterrace atomic planes.

2. Vicinal of Cu-Pd(17%) (110)

In order to assess the generality of the emergence of APB's at vicinal surfaces we have further investigated by STM a vicinal (miscut 1.8°) of Cu-Pd (17%) (110) after short ordering 1 h, ($\Delta T = 15$ K) (the sample we previously studied by He diffraction[24]). STM images show that APB's emerge very much as on the (1,1,11) surface. Emergence of APB's is thus evidenced on one other surface and for a miscut much lower than for (1,1,11) surfaces.

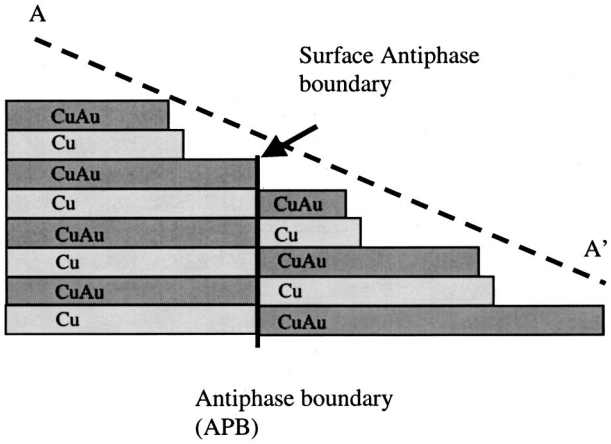

FIG. 6. Bulk cross section across a SAPB (perpendicular to the surface and along the segment AA' defined in Fig. 4).

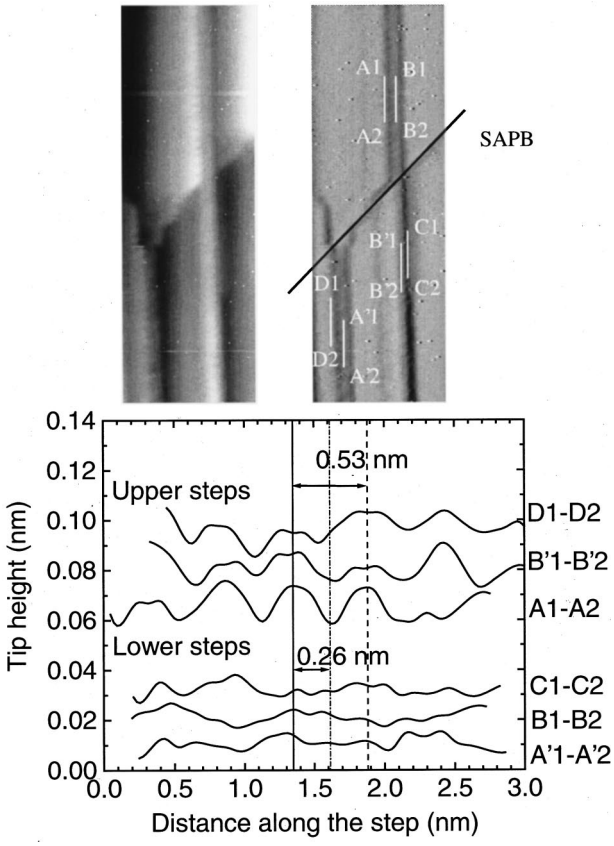

FIG. 7. Top: 6.8 nm×20 nm STM image and $\partial z/\partial x$ image of the same area. One SAPB where paired steps separate crosses the picture. Bottom: tip-height modulation along step edges (white bars on the $\partial z/\partial x$ image indicate the position of each cross section). The wavelength of the tip-height modulation along upper step edges is $2a$. The amplitude of the tip-height modulation at lower step edges is smaller. Across the SAPB the tip-height modulation at A and B step edges changes consistently with a change in the nature of the corresponding atomic planes ($A1$-$A2$ and $B'1$-$B'2$, CuAu; $A'1$-$A'2$ and $B1$-$B2$, Cu).

D. Vicinal surfaces: Conclusion

Chemical ordering at vicinal surfaces of the two alloys considered appears very similar. The different behavior of

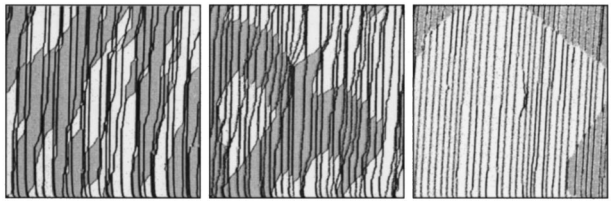

FIG. 8. $\partial z/\partial x$ images (102.4 nm×102.4 nm) of Cu_3Au (1,1,13) ($T = 293$ K) after, from left to right, 5 min, 4 h, and 18 h annealing at $T_c - 20$ K. White and gray colored terraces are for the two possible surface domains.

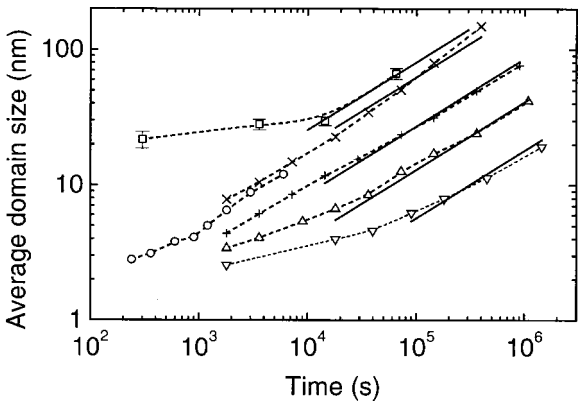

FIG. 9. Characteristic domain size Λ as a function of annealing time. (□) Surface domain size measured from STM images according to Eq. (1) for ordering at $\Delta T = T_c - T = 20$ K. Taking into account that only two APB's out of three are observed, data have been multiplied by a factor 2/3 for comparison with bulk data. Bulk domain characteristic size measured by x-ray diffraction by Poquette and Mikkola (Ref. 4): $\Delta T = (\nabla)90$, (△) 65, (+) 40, and (×) 15 K. (○) Same measured by Hashimoto, Nishimura, and Takeuchi (Ref. 5) at $\Delta T = 5$ K. (——) $t^{1/2}$ law according to AC (Ref. 1).

their bulk APB's makes the present comparison crucial to draw firm conclusions on surface ordering at vicinal surfaces. Emergence of APB's appears as a common property of the vicinals studied. In the late stage of surface ordering on vicinals, the observation of similar bulk and surface characteristic lengths for ordered domains [Cu_3Au and Cu-Pd(17%)] and of similar activation energies for bulk and surface domain coarsening [Cu-Pd(17%)] indicates that the late stage of surface ordering is driven by bulk APB dynamics. The observation of step pairing and the evolution of SAPB's on $Cu_3Au(1,1,13)$ clearly shows that APB's emerge at the surface, in strong contrast with the fact that these APB's do not emerge on the (001) surface of the same alloy.[10] It turns out that the emergence of APB's at the surface is made possible by the presence of a high density of steps and thus depends on surface orientation.

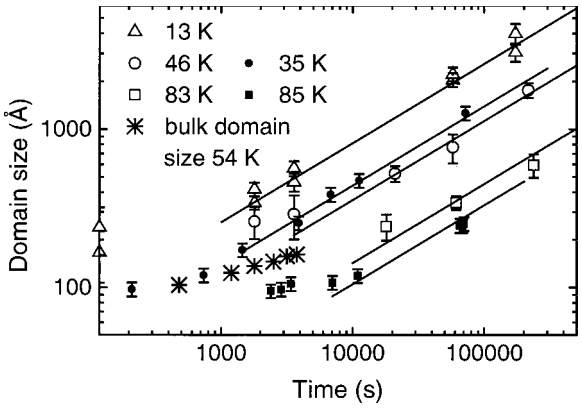

FIG. 10. Cu-Pd(17%) (1,1,11). Average domain size versus ordering time for various $\Delta T = T_c - T$ temperatures. Open symbols, STM measurements; full symbols, He diffraction measurements. (*) Bulk size domain measured by *in situ* x-ray diffraction. (——) $t^{1/2}$ law according to AC (Ref. 1).

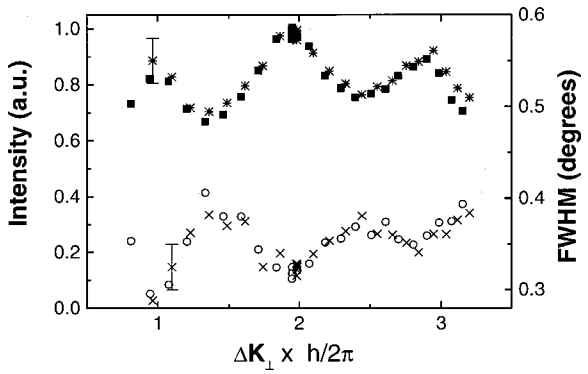

FIG. 11. Cu-Pd(17%) (001). Intensity and width of the (0,0) specular peak as a function of $\Delta \mathbf{K}_\perp$. Intensities for $T = (\blacksquare)823$ K $> T_c$ and (*)753 K $< T_c$ have been corrected for thermal attenuation (Debye-Waller factor). Full width at half maximum (FWHM) of the specular peak for $T = (\bigcirc)823$ K and (×) 753 K.

IV. Cu-Pd(17%) (001)

In order to assess the generality of the contrasting behaviors of the (001) and vicinal surfaces in the emergence of APB's, we have investigated the Cu-Pd(17%) (001) surface by He diffraction and STM. On such a low-index surface, wide terraces with a high-energy terminal plane [Cu-Pd for Cu-Pd(17%)] cannot exist. Upon ordering, extra single steps are thus expected to be formed along with the emergence of APB's, in such a way that all terraces are pure Cu planes. Note that only APB's for which the translation vector has a nonzero component in the [001] direction (i.e., including a shift of the η_z component of the order parameter) induce a shift in the z direction of the Pd concentration component.

In the He diffractometer, the sample azimuth is chosen in such a way that the [110] direction is in the incidence plane. Incidence angles θ_i are measured with respect to the surface normal. As in Cu(001), the only observable diffraction peak is the specular and the intensity of other diffraction peaks is below our detection limit ($I/I_0 = 2 \times 10^{-6}$). The corrugation of the terraces is thus very small, as expected for a pure Cu plane. The (0,0) peak shape and intensity were recorded versus $\varphi_h(\Delta \mathbf{K}_\perp)$ (i.e., versus incident angle θ_i) for $T = 823$ K, i.e., above T_c. As shown in Fig. 11, the intensity and the peak width oscillate versus $\Delta \mathbf{K}_\perp$, thus showing that residual steps are present on our sample. We have used these results to determine precisely the in-phase (P) and out-of-phase (AP) kinematic conditions. From the period of the width and intensity oscillations, one finds that the step height is 0.183 nm, in agreement with the elementary step height, so that most steps are single. The amplitude of the width oscillations can be related to the step density,[28] and from our measurement the average terrace size is of the order of 100 nm. After 24 h ordering at $T = T_c - 25$ K, the very same peak width and intensity oscillations are measured (at $T = 753$ K). In such conditions, the characteristic size of chemically ordered domains measured on vicinal surfaces of the same alloy would be greater than 100 nm.

We then measured the peak width and intensity of the specular peak during the ordering process at $T_c - 25$ K, after a rapid quenching from $T = 823$ K. Measurements were done

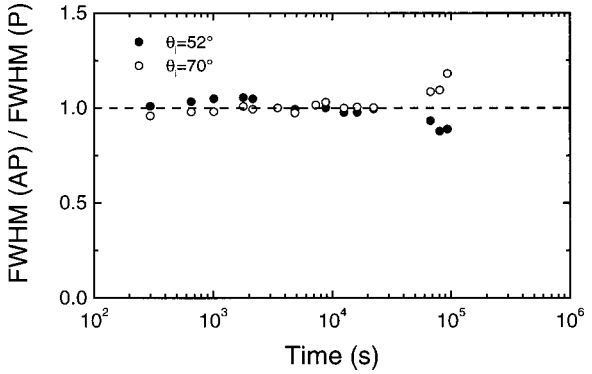

FIG. 12. Cu-Pd(17%) (001). Ratio of the FWHM of the specular peak for $\theta_i = 70°$ and 52° (close to the AP condition) to the FWHM measured for $\theta_i = 60°$ (close to the P condition) versus ordering time at $T_c - 25$ K.

for $\theta_i = 60°$ (close to the P condition) and $\theta_i = 70°$ and 52° (close to the AP condition). The width ratio between AP and P conditions remains constant during ordering (see Fig. 12); this indicates that no extra steps are formed. In contrast, an evolution of the width of He diffraction peaks in AP conditions on the (1,1,11) vicinal surface is clearly observed at $T_c - 35$ K.[12] This shows that the surface morphology of the (001) surface is not affected by bulk chemical ordering and that no APB's emerge at the surface.

STM images were taken on the very same (001) sample at room temperature after 1 h annealing at $T = 733$ K $= T_c - 45$ K, for which the size of surface domains on the (1,1,11) surface is of the order of 30 nm. Scarce residual steps are observed, defining terraces wider than 100 nm. The step density is obviously much lower than expected from the SAPB density measured on the vicinal. At some places on our sample, small bunches of steps can be observed. Paired steps, as well as single steps, are visible, as shown in the image of Fig. 13. It is remarkable that on the left part of the image paired steps separate in the same way as on vicinal surfaces. In this area, upper and lower terraces are not affected. These observations are in good agreement with our He diffraction experiment and thus consistently show that the (001) surface morphology is not affected by chemical ordering.

The present results are fully consistent with previous investigations on surface chemical ordering in Cu_3Au (001) by x-ray diffraction,[10] STM,[29] and He diffraction.[30,31] On Cu_3Au (001), Mannori *et al.*[30,31] observed He diffraction peaks for $T < T_c$, in addition to the specular, which indicates in agreement with their low-energy ion scattering LEIS study that the terminal plane is $c(2\times2)$Cu-Au ordered. Furthermore, they observed oscillations of the specular intensity as a function of incidence angle that they attributed to the presence of a low density of residual steps. From data analysis, they concluded that single steps (and not only double steps) are present after 1 h ordering at $T_c - 23$ K with a density such that 95% of the surface (within the transfer length of their diffractometer) is at the same level. In a more quantitative STM experiment, Lin *et al.*[29] observed that the step density on a Cu_3Au (001) sample does not depend on the ordering

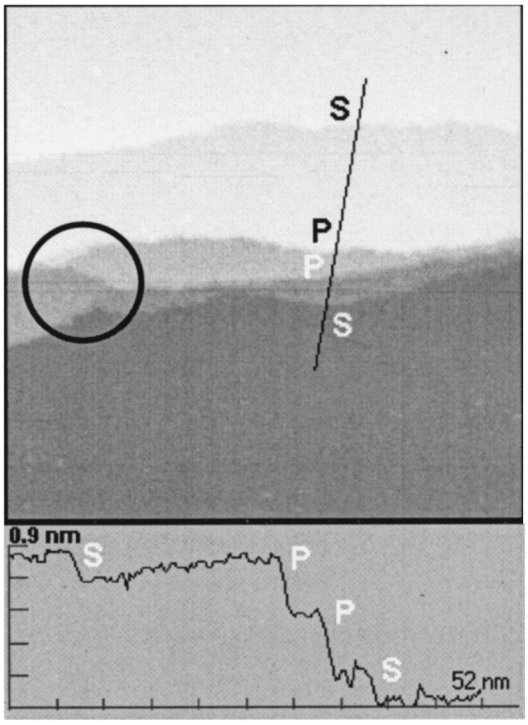

FIG. 13. 90 nm×90 nm STM image of Cu-Pd(17%) (001) (after 1 h annealing at $T_c - 45$ K). The surface profile along the indicated line shows that paired (*P*) and single (*S*) steps are present. In the area within the circle, paired steps separate to be paired differently whereas adjacent terraces appear unaffected.

time even after a rapid quenching. These experiments together with the x-ray study on Cu_3Au (001),[10] and our observations on Cu-Pd(17%) (001), show that the (001) surfaces of the two alloys have similar behaviors: a low single-step density is observed after short ordering and this density remains constant during chemical ordering. The emergence of APB's would induce a high and slowly decaying single-step density in order to preserve the preferred surface termination, which is not observed. This allows us to conclude that APB's with a component of the translation vector perpendicular to the surface plane do not emerge on the (001) surface.

V. CHEMICAL ORDERING AT SURFACES: CONCLUSION

Previous experiments[10,12] and our present observations on low-index and vicinal surfaces show that the process of chemical ordering alters the morphology of vicinals while it does not affect that of close-packed surfaces. Based on this result, the ordering process at surfaces may be described as follows.

Above T_c, the bulk is disordered and, due to surface segregation, the η_z component of the order parameter is nonzero at the surface. This reflects the oscillatory concentration profile in the direction normal to terraces [see Fig. 14(a)]. APB's localized in the subsurface region are thus present below each step. As shown by Reichert *et al.*,[10] this preexisting order at the surface acts as a template for surface

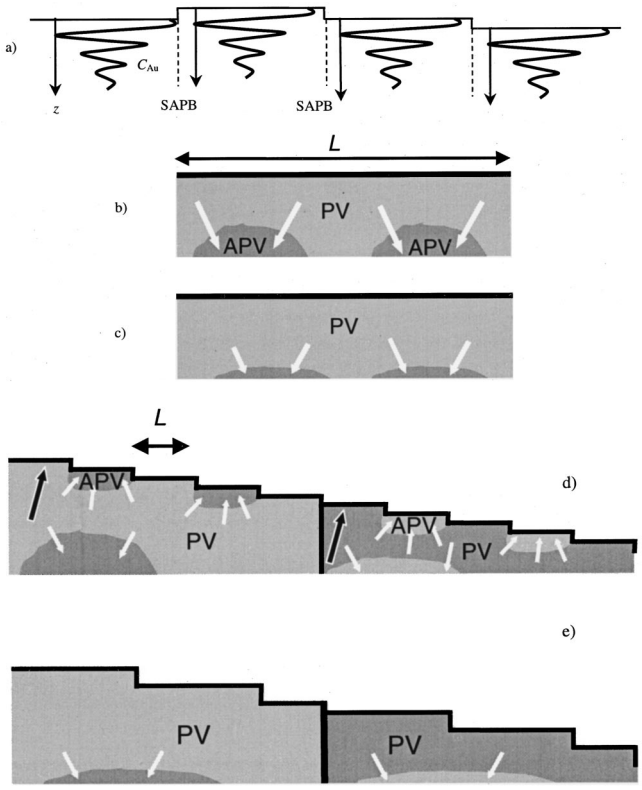

FIG. 14. (a) Disordered crystal ($T > T_c$). Surface segregation induces an oscillatory concentration profile underneath each terrace (Ref. 10). Evanescent surface antiphase boundaries (dashed lines) are present and pinned at step edges. The nonzero component of the order parameter η_z in the surface vicinity acts as a template for surface chemical ordering. (b) Chemical ordering for $L \gg \Lambda$. PV (APV) designates domains with in-phase (out-of-phase) η_z component with respect to the surface order. APV's cannot emerge at the surface whereas PV's merge with the surface domain. (c) Upon aging, the thickness of the ordered surface layer increases. Note that only two APB's out of three (for which the translation vector has a nonzero *z* component, i.e., separating PV's and APV's are shown. (d) After long ordering ($L \ll \Lambda$), wide bulk domains (PV or APV) are formed. Small domains beneath one terrace out of two are formed. (e) These domains shrink and a paired-step structure results.

ordering below T_c [see Fig. 14(b)]. Variants compatible with the surface termination are thus selected in this manner. Simultaneously, small domains belonging to the four possible variants are formed within the bulk. The η_z component is in phase with the ordered surface layer for only two variants (PV) and is in phase opposition for the two others (APV). PV's merge with the surface domain and APB's (with a component of the translation vector perpendicular to the terrace planes) are formed between APV's and the surface ordered layer. In other words, APB's resulting from the bulk ordering process cannot emerge at the surface. The APB's thus formed necessarily exhibit a *convex* curvature toward the bulk [Fig. 14(b)]. Within the AC process, small domains shrink, leading to an increase of the average domain size and a reduction of the curvature of APB's. The thickness of the ordered surface layer increases in that way (*surface-driven ordering*) [Fig. 14(c)]. This explains the observed nonemergence of APB's at (001) surfaces. Experimental observations on flat surfaces consistently show that no steps are formed upon ordering and that the surface keeps its preferential termination. This is expected to occur beneath every terrace of a vicinal surface in the early ordering stage.

As the aging proceeds for vicinal surfaces, bulk domains become wider than the step-step distance *L*. The APB's pinned at steps then merge and exhibit a curvature *toward the surface* [see Fig. 14(c)]. According to the AC process, these domains encapsulated in a wider domain must subsequently shrink and in agreement with our experimental observations on vicinal surfaces double steps are formed in such a way that the preferential termination is obtained for all terraces (*bulk-driven ordering*). Thus, the contrasting behavior between flat and vicinal surfaces suggests that ordering occurs in two steps. For short ordering times, *L* is much larger than Λ and surface ordering prevails. For long aging times, *L* becomes smaller than Λ and emerging bulk domains impose surface chemical order.

In conclusion, we have shown that the influence of chemical order on surface morphology is different for flat and vicinal surfaces of $L1_2$ alloys. This is valid for the two alloys investigated although their bulk APB's have very different behaviors. The absence of step formation upon ordering on flat surfaces confirms the conclusion of Reichert *et al.*[10] that surface segregation imposes the surface η_z order-parameter component. For vicinal surfaces, for which *L* is much lower than Λ, step pairing allows reducing the surface energy and the surface morphology is driven by bulk chemical order as shown by the emergence of bulk APB's.

ACKNOWLEDGMENTS

The authors thank P. Lavie and F. Merlet (CEA) for technical assistance in He and STM experiments, D. Regent (ONERA) for preparation of the single crystals, and F. Savoy (ONERA) for the cutting of the samples.

*Author to whom correspondence should be addressed. Electronic address: lbarbier@cea.fr

[1] S. M. Allen and J. W. Cahn, Acta Metall. **27**, 1085 (1979).
[2] O. G. Mouritsen, Int. J. Mod. Phys. B **4**, 1925 (1990).
[3] J. D. Gunton, M. San Miguel, and P. S. Sahni, Phase Transit. **8**, 267 (1983).
[4] G. E. Poquette and D. E. Mikkola, Trans. Metall. Soc. AIME **245**, 743 (1969).
[5] T. Hashimoto, K. Nishimura, and Y. Takeuchi, Phys. Lett. **65A**, 250 (1978).
[6] R. F. Shannon, S. E. Nagler, C. R. Harkless, and R. M. Nicklow, Phys. Rev. B **46**, 40 (1992), and references therein.
[7] S. Duval, S. Chambreland, A. Loiseau, and D. Blavette, J. Mater. Res. **13**, 1502 (1998).
[8] H. Dosch, L. Mailänder, A. Lied, J. Peisl, F. Grey, R. L. Johnson, and S. Krummacher, Phys. Rev. Lett. **60**, 2382 (1988).

[9] H. Dosch, L. Mailänder, H. Reichert, J. Peisl, and R. L. Johnson, Phys. Rev. B **43**, 13 172 (1991).
[10] H. Reichert, P. J. Eng, H. Dosch, and I. K. Robinson, Phys. Rev. Lett. **78**, 3475 (1997).
[11] E. G. McRae and R. A. Malic, Phys. Rev. Lett. **65**, 737 (1990).
[12] S. Goapper, L. Barbier, B. Salanon, A. Loiseau, and X. Tolleres, Phys. Rev. B **57**, 12 497 (1998).
[13] Ch. Ricolleau, A. Loiseau, F. Ducastelle, and R. Caudron, Phys. Rev. Lett. **68**, 3591 (1992).
[14] S. B. Rivers, W. N. Unertl, H. H. Hung, and K. S. Liang, Phys. Rev. B **52**, 12 601 (1995).
[15] T. M. Buck, G. H. Weatley, and L. Marchut, Phys. Rev. Lett. **51**, 43 (1983).
[16] L. Potez and A. Loiseau, Interface Sci. **2**, 7 (1994).
[17] M. J. Hÿtch and L. Potez, Philos. Mag. A **76**, 1119 (1997).
[18] I. K. Robinson and P. J. Eng, Phys. Rev. B **52**, 9955 (1995).
[19] J. W. Cahn, Scr. Metall. **14**, 93 (1980).
[20] F. A. Shunk and M. Hansen, *Constitution of Binary Alloys* (McGraw-Hill, New York, 1969).
[21] E. Le Goff, Ph.D. thesis, University of Paris VI, 1999; E. Le Goff, L. Barbier, A. Loiseau, and B. Salanon, Surf. Sci. **466**, 73 (2000).
[22] S. Goapper, L. Barbier, and B. Salanon, Surf. Sci. **364**, 99 (1996); **409**, 81 (1998).
[23] L. Barbier, S. Goapper, B. Salanon, R. Caudron, A. Loiseau, J. Alvarez, S. Ferrer, and X. Torrelles, Phys. Rev. Lett. **78**, 3003 (1997).
[24] L. Barbier, B. Salanon, and A. Loiseau, Phys. Rev. B **50**, 4929 (1994).
[25] T. M. Buck, G. H. Weatley, and L. Marchut, Phys. Rev. Lett. **51**, 43 (1983).
[26] H. Niehus and C. Achete, Surf. Sci. **289**, 19 (1993).
[27] S. Goapper, Ph.D. thesis, University of Marne la Vallée, France, 1998.
[28] J. Lapujoulade, Surf. Sci. **108**, 526 (1981).
[29] M. T. Lin, J. Shen, W. Kuch, H. Jenniches, M. Klaua, C. M. Schneider, and J. Kirschner, Surf. Sci. **410**, 290 (1998).
[30] C. Mannori, T. Scimia, P. Cantini, S. Terrini, M. Canepa, and L. Mattera, Surf. Sci. **433-435**, 307 (1999).
[31] C. Mannori, G. Boato, M. Canepa, P. Cantini, L. Mattera, and S. Terrini, Europhys. Lett. **45**, 686 (1999).